LAMINAR-TURBULENT TRANSITION CORRELATIONS IN SUPERSONIC / HYPERSONIC FLAT PLATE FLOW

G.A. Simeonides*
***Hellenic Aerospace Industry, P.O. Box 23, GR-32009 Schimatari, Greece**
and Dept. Mechanical and Aeronautical Engineering, Univ. Patras, Greece

Keywords: *transition, supersonic, hypersonic, flat plate, bluntness*

Abstract

Flat plate transition data in the supersonic and hypersonic flow regimes, is manipulated to provide simple transition prediction formulations. The extensive data set, which comes from a significant number of experiments with finite leading edge thickness models in various wind tunnels, has been previously assembled in a database, and elaborated to reveal the primary correlation parameters.

The data is organized in a convenient way for regression analysis and the establishment of simple mathematical correlation forms. Noting the significant size of the database, and the successful correlation of the majority of the data, practicable flat plate transition prediction tools are proposed and their ranges of applicability identified. The proposed formulations capture, among other things, transition reversal at strong bluntness conditions, while at weak bluntness conditions there are indications of important initial disturbance and receptivity effects, which are not included in the present analysis.

List of symbols

A	constant of proportionality
b	leading edge thickness
C	Chapman-Rubesin linear viscosity law constant, $= \frac{T_\infty}{T}\frac{\mu}{\mu_\infty}$
k	exponent
M	(free-stream) Mach number
Re_b	(leading edge) bluntness Reynolds number, based on free-stream flow conditions and the leading edge thickness, $= \frac{\rho_\infty u_\infty b}{\mu_\infty}$
Re_{unit}	unit Reynolds number (per meter, unless otherwise stated), based on free-stream flow conditions, $= \frac{\rho_\infty u_\infty}{\mu_\infty}$
Re_x	Reynolds number based on free-stream flow conditions and the distance from the leading edge, $= \frac{\rho_\infty u_\infty x}{\mu_\infty}$
Re_{xtrans}	transition Reynolds number based on free-stream flow conditions and the distance from the leading edge to the location of transition onset, $= \frac{\rho_\infty u_\infty x_{tr}}{\mu_\infty}$
T	temperature
u	stream-wise velocity
x	stream-wise distance from the leading edge

Greek symbols

β	bluntness parameter, $= \frac{M^2}{(x/b)^{2/3}}$
μ	viscosity
ρ	density
$\bar{\chi}$	viscous interaction parameter, $= \frac{M^3}{\sqrt{\mathrm{Re}_x}}\sqrt{C}$

Subscripts

tr	transition onset location
w	wall conditions
0	total (stagnation) flow conditions

1 Introduction

A supersonic / hypersonic flow flat plate transition onset database has been assembled in [1,2] including data from [3-13] and covering a range in free-stream Mach number, M, between 2 and 8, free-stream unit Reynolds number, Re_{unit}, between 2 million and 75 million per meter, and leading edge thickness, b, between 2.5 μm and 2 mm. The corresponding free-stream-based leading edge bluntness Reynolds numbers, Re_b, range between 20 and 100,000, while transition is found to occur at free-stream-based Reynolds numbers (based on transition onset location), Re_{xtrans}, between 0.7 and 18 million or at values between 10 and 110,000 for the transition onset location normalized by the leading edge thickness, (x_{tr}/b).

The majority of the data has been collected under near-adiabatic wall conditions, with the exception of the cold wall Mach 6 and 7 data of [3-7], where the wall-to-total temperature ratio, T_w/T_0, was in the vicinity of 0.5. With regard to the Mach 8 data of [10,11], the data of [10] are stated to have been collected at the radiation-equilibrium wall temperature (some 20% lower than the adiabatic wall temperature), while in the case of [11] the surface temperature, T_w, was maintained at approximately 0.4 the flow total temperature, T_0. In fact, the Mach 8 data of [10,11] were taken on hollow cylinder models, rather than actual flat plates.

The assembled data has been successfully correlated in [2], only after it was distinguished on the basis of a pressure field criterion into two categories:

- "viscous-dominated" transition data, where transition occurs in a viscous interaction dominated environment, and
- "bluntness-dominated" transition data, where transition occurs in a leading edge bluntness dominated environment.

The selection criterion proposed for this data distinction in [2] is actually the ratio of the bluntness-induced pressure increment parameter, β, to the viscous interaction parameter, $\bar{\chi}$, both evaluated at the measured location of transition onset:

$$\left(\frac{\beta}{\bar{\chi}}\right)_{tr} = \frac{\sqrt{\mathrm{Re}_{xtrans}}}{M\left(x_{tr}/b\right)^{2/3}} = \frac{\sqrt{\mathrm{Re}_{\infty,b}}}{M\left(x_{tr}/b\right)^{1/6}} \qquad (1)$$

where the Chapman-Rubesin constant, C, is neglected (taken as unity). Then:

- the pressure increment due to bluntness is equal to the pressure increment due to viscous interaction when the ratio $(\beta/\bar{\chi}) \cong 1.9$
- bluntness effects on the pressure field at the transition location are more important than viscous effects when $(\beta/\bar{\chi})_{tr} > 1.9$ (bluntness-dominated transition)
- viscous effects are more important than bluntness effects when $(\beta/\bar{\chi})_{tr} < 1.9$ (viscous-dominated transition).

The good correlation of flat plate transition measurements that resulted from such a distinction to viscous- and bluntness-dominated data [2] is demonstrated in Figs. 1 and 2. One sole exception is found in Fig. 1, where the Mach 8 data of [10,11] exhibits a more stable behaviour and significantly higher transition Reynolds numbers than the rest of the viscous-dominated data.

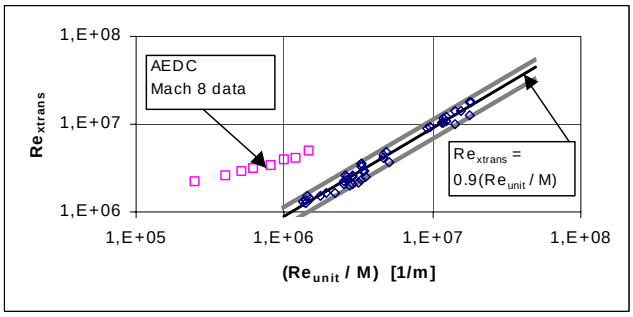

Fig. 1 Viscous-dominated transition data correlation [2], and mathematical representation

In what follows, regression analysis is applied to the data of Figs. 1 and 2 and, with some further elaboration, simple mathematical forms suitable for flat plate transition prediction are proposed and their ranges of applicability identified.

2 Data Correlation and Regression Analysis

2.1 Weak Bluntness Data

The weak bluntness or viscous-dominated transition data of Fig. 1 include Mach 3.5 data from the NASA Quiet Tunnel [8] with leading edge thicknesses of 2.54 μm, 12.7 μm and 22.86 μm, Mach 6 data from VKI [5-7] with leading edge thicknesses of 14 μm, 34 μm, 54 μm and 80 μm, and Mach 7 data from CERT-ONERA [3,4] with a leading edge thickness of 12 μm. The Mach 8 data of [10,11], with leading edge thicknesses of 50.85 and 102 μm, also belong to the viscous-dominated category, according to the pressure field selection criterion defined hereabove, but as previously noted this high Mach number data appears significantly more stable than the rest of the "weak bluntness" data in the presentation of Fig. 1.

With reference to Fig. 1, the weak bluntness data (excluding the Mach 8 data of [10,11]) exhibit a quasi-linear correlation between the transition Reynolds number, Re_{xtrans}, and the ratio of unit Reynolds number to Mach number, (Re_{unit}/M). Regression analysis yields the following correlation form:

$$\mathrm{Re}_{xtrans} = 0.9\,\frac{\mathrm{Re}_{unit}}{M} \qquad (2)$$

The above eq. (2) is also plotted in Fig. 1, together with a +/-25% uncertainty band. All data in this category (excluding the Mach 8 data) falls within this +/-25% band.

2.2 Modest Bluntness Data

With reference to Fig. 2, the bluntness-dominated transition data is distinguished in two sub-categories exhibiting two distinct trends:

- on the left hand side of Fig. 2 and at values of (Re_b/M^2) less than approximately 1000, the modest bluntness data trend shows a relatively mild negative inclination
- at values of (Re_b/M^2) greater than approximately 1000, the strong bluntness data trend shows an increased negative inclination.

The modest bluntness data of Fig. 2 include the Mach 7 measurements from CERT-ONERA [3,4] with a leading edge thickness of 200 μm, the Mach 3 data of [9] with leading edge thicknesses of 20, 50 and 100 μm (and some with 180 μm), as well as the Mach 2-4 data from [9] with a 100 μm leading edge (excluding some Mach 2 and 2.5 data), the Mach 3-5 data of [10] with leading edge thicknesses of 75 and 200 μm, the Mach 3 data of [12] with a leading edge thickness of 150 μm, and the Mach 2-4 data of [13] with leading edge thicknesses of 25-200 μm.

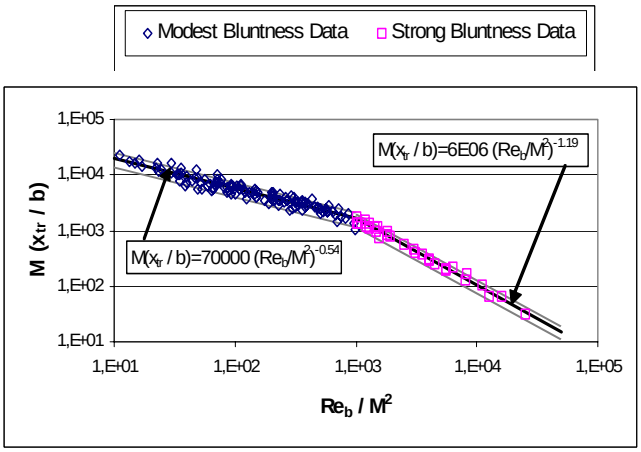

Fig. 2 Bluntness-dominated transition data correlation [2], and mathematical representation

On the basis of regression analysis, the modest bluntness data of Fig. 2 exhibits the following correlation:

$$M\,\frac{x_{tr}}{b} = 70000\left(\frac{\mathrm{Re}_b}{M^2}\right)^{-0.54} \qquad (3)$$

which is plotted in Fig. 2, together with a +/-30% band. The majority of modest bluntness transition data falls within this band.

Manipulation of eq. (3) yields an alternative correlation form, in terms of transition Reynolds number, as follows:

$$\mathrm{Re}_{xtrans} = 70000\,M^{0.08}\,\mathrm{Re}_b^{0.46} \qquad (4)$$

which shows a weak dependence of transition Reynolds number on Mach number and a primary dependence on leading edge bluntness Reynolds number, Re_b, for this category of modest bluntness transition data.

A plot of the transition Reynolds number, Re_{xtrans}, versus the primary dependence parameter Re_b is shown in Fig. 3 for modest bluntness data only.

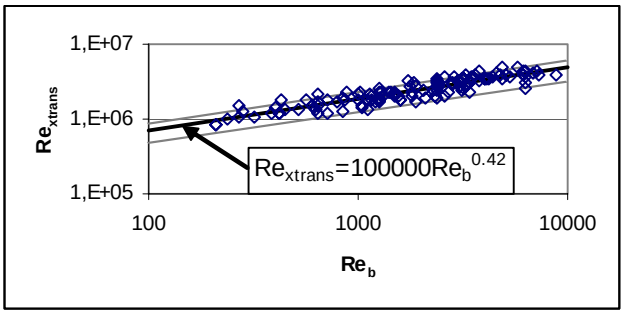

Fig. 3 Modest bluntness data simplified correlation

Application of regression analysis to the data of Fig. 3 yields an approximate correlation for modest bluntness transition Reynolds number, which is independent of the Mach number, in the form:

$$\mathrm{Re}_{xtrans} = 100000\,\mathrm{Re}_b^{0.42} \qquad (5)$$

Again, the majority of the data in Fig. 3 falls within a +/-30% band.

2.3 Strong Bluntness Data

The strong bluntness data on the right hand side of Fig. 2 include the Mach 3 data of [9] with leading edge thicknesses of 180 (some), 440 and 710 μm, as well as some Mach 2 and 2.5 data from [9] with a 100 μm leading edge, and the Mach 2-4 data of [13] with leading edge thicknesses of 1 and 2 mm.

With reference to Fig. 2, the strong bluntness data correlates according to:

$$M\frac{x_{tr}}{b} = 6\cdot 10^6\left(\frac{\mathrm{Re}_b}{M^2}\right)^{-1.19} \qquad (6)$$

All data in this category falls within a +/-25% uncertainty band of eq. (6).

Manipulation of eq. (6) yields an alternative correlation form, in terms of transition Reynolds number, as follows:

$$\mathrm{Re}_{xtrans} = 6\cdot 10^6\, M^{1.38}\,\mathrm{Re}_b^{-0.19} \qquad (7)$$

which shows, in this case, a relatively weak dependence of transition Reynolds number on leading edge bluntness Reynolds number, Re_b, and a primary dependence on free-stream Mach number.

Plotting the strong bluntness data in the form of transition Reynolds number, Re_{xtrans}, versus Mach number, M, that is neglecting the mild dependence on leading edge bluntness Reynolds number, Re_b, in this case, yields the result shown in Fig. 4.

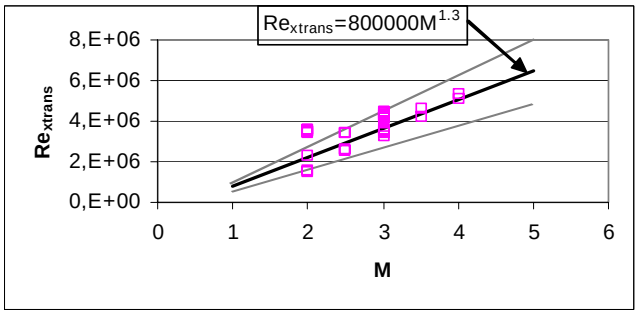

Fig. 4 Strong bluntness data simplified correlation

Here, the Mach number dependence of the transition Reynolds number is represented by:

$$\mathrm{Re}_{xtrans} = 800000M^{1.3} \qquad (8)$$

although the residual Re_b dependence remains evident in the limited (with respect to Mach number range) data set of Fig. 4. For reference, a +/-25% band is also shown in Fig. 4 around the plot of eq. (8).

3 Ranges of Applicability

3.1 Weak-to-Modest Bluntness Threshold

The boundary between weak and modest bluntness transition data summarized above can be determined by substituting eq. (3) into eq. (1) and manipulating for the condition that $(\beta/\overline{\chi}) \cong 1.9$. In fact, solving eq. (1) for Re_b as a function of M, the threshold boundary between weak and modest bluntness transition is obtained as:

$$\mathrm{Re}_b \cong 70M^{1.7} \qquad (9)$$

Theoretically, therefore, when $\mathrm{Re}_b \geq 70M^{1.7}$, flat plate boundary layer transition can be expected to be bluntness-dominated and, thus, characterized by the correlation of eqs. (3) and (4), or the simplified form of eq. (5)[1]. When $\mathrm{Re}_b \leq 70M^{1.7}$, then flat plate boundary layer transition can be expected to be viscous-dominated and, thus, characterized by the correlation of eq. (2).

It must be noted, however, that in practice the boundary between viscous- and bluntness-dominated transition is not as precise as eq. (9). This has already been manifested above by the failure of the Mach 8 data of [10,11] to correlate with the rest of the viscous-dominated transition data of Fig. 1, although in terms of the criteria of both eqs. (1) and (9), this data falls well within the viscous-dominated regime. Overall, the available data indicates that there is more of a buffer zone between viscous- and bluntness-dominated transition, rather than a clear threshold between the two categories. This matter is further elaborated in section 4 below.

3.2 Modest-to-Strong Bluntness Threshold

The boundary between the modest and strong bluntness sub-categories of the bluntness-dominated transition data may be established by equating eqs. (3) and (6), and solving for the leading edge bluntness Reynolds number, Re_b, as a function of free-stream Mach number, M.

The theoretical threshold boundary between modest and strong bluntness transition is then:

$$\mathrm{Re}_b \cong 940M^2 \qquad (10)$$

which is fairly close to the $(Re_b/M^2)=1000$ criterion used to distinguish the data of Fig. 2 and establish the modest and strong bluntness correlation forms, eqs. (3) and (6), by regression.

Consequently, when $\mathrm{Re}_b \geq 1000M^2$, flat plate boundary layer transition is characterized by strong bluntness effects and, thus, described by the correlation of eqs. (6) and (7), or the less accurate form of eq. (8). When $\mathrm{Re}_b \leq 1000M^2$, then flat plate boundary layer transition is characterized by modest bluntness effects and, thus, described by the correlation of eqs. (3) and (4) or the simplified version of eq. (5).

Although the boundary between modest and strong bluntness transition data is definitely more precise than the weak-to-modest bluntness data boundary discussed above, the availability of a rather limited amount of strong bluntness data, illustrated in Fig. 4, should be noted.

4 Further Data Elaboration and Alternative Correlation Forms

4.1 Re-evaluation of Weak Bluntness Data

The weak bluntness (viscous-dominated) transition data of Fig. 1 deserve further attention, not only because of the fact that the Mach 8 data of [10,11] does not correlate with the remaining viscous-dominated data in Fig. 1, but also because the resulting correlation, eq. (2), exhibits a rather peculiar destabilizing influence of increasing Mach number.

It is recalled that eq. (2) results from regression analysis of the Mach 3.5 NASA quiet tunnel data of [8], the Mach 6 VKI data of [5-7] and the (small bluntness) Mach 7 ONERA data of [3,4]. The Mach 8 AEDC data of [10,11] has been excluded from the correlation of eq. (2). Consequently, the inversely proportional relation of transition Reynolds number, Re_{xtrans}, to the Mach number, M, in eq. (2) is significantly influenced by the nature (and "quietness") of the Mach 3.5 data of [8], while it is strongly contradicted by the excluded Mach 8 data of [10,11].

This observation is further exemplified in the plot of Re_{xtrans} versus Re_{unit} shown in Fig. 5, where the weak bluntness data, including the Mach 8 data of [10,11], exhibits no unique Mach number trend.

[1] Provided of course that leading edge bluntness remains within the range of applicability of the modest bluntness correlation, i.e. it is not "strong".

It is likely, therefore, that in cases of weak bluntness (viscous-dominated) transition, the initial disturbance environment and the boundary layer receptivity mechanism are of outmost importance to the evolution of the phenomenon, thus prohibiting a generalized correlation in the present macroscopic forms which exclude such parameters.

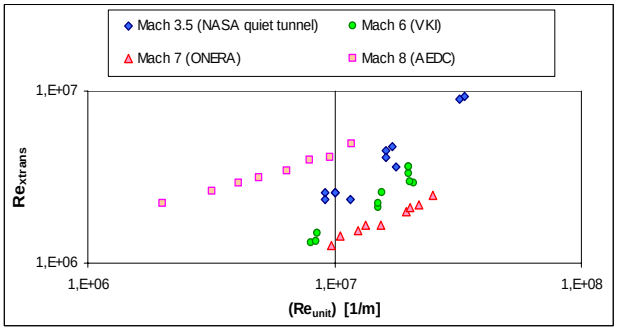

Fig. 5 Weak bluntness data presentation

Nevertheless, each individual weak bluntness data set in Fig. 5 exhibits a Re_{xtrans} versus Re_{unit} relation of a form that is well known in the literature [10,11,14-16]:

$$\mathrm{Re}_{xtrans} = A\,\mathrm{Re}_{unit}^{k} \qquad (11)$$

This relation is only weakly dependent on leading edge thickness[2] in Fig. 5. Within the limitation of the small number of weak bluntness data available in Fig. 5, the exponent, k, in eq. (11) is found to depend on Mach number according to:

$$k = 0.2045 + 0.3918M - 0.0457M^2 \qquad (12)$$

while a simple relation of the constant of proportionality, A, to Mach number has not been established, again indicating the likely influence of parameters not included in the present database (e.g. initial disturbance environment and boundary layer receptivity).

4.2 Combined Weak and Modest Bluntness Data Correlation

If the entirety of the data is plotted in the "bluntness-dominated" presentation form of Fig. 2 (Mx_{tr}/b versus Re_b/M^2), it is seen in Fig. 6 that all weak bluntness data, with the exception of the NASA quiet tunnel data of [8], correlates reasonably well with the modest bluntness data[3].

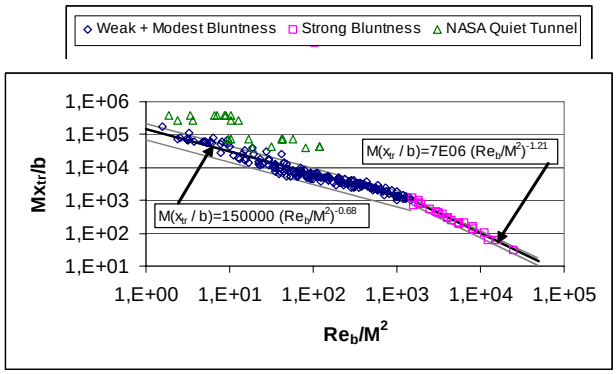

Fig. 6 Data correlation – all data

Regression analysis applied in Fig. 6 to the combined weak and modest bluntness data (but excluding, in this case, the quiet tunnel data of [8] and, of course, the strong bluntness data) yields the subsequent correlation form:

$$M\frac{x_{tr}}{b} = 150000\left(\frac{\mathrm{Re}_b}{M^2}\right)^{-0.68} \qquad (13)$$

which is shown in Fig. 6 with a +/-50% uncertainty band to encompass the majority of the subject data.

Alternatively, eq. (13), may take the form:

$$\mathrm{Re}_{xtrans} = 150000M^{0.36}\,\mathrm{Re}_b^{0.32} \qquad (14)$$

which exhibits a weaker dependence on bluntness Reynolds number than eq. (4) (established for purely modest bluntness data), and a much stronger dependence on Mach number. The latter effect is intuitively reasonable, as it shows a (mild) stabilizing effect of increasing Mach number.

[2] It is recalled that the Mach 3.5 NASA quiet tunnel data includes leading edge thicknesses of 2.54, 12.7 and 22.86 μm, the Mach 6 VKI data includes leading edge thicknesses of 14, 34 and 54 μm, and the Mach 8 AEDC data includes leading edge thicknesses of 50.85 and 102 μm. The Mach 7 ONERA data in Fig. 5 correspond to a 12 μm leading edge.

[3] Amongst the NASA data, the points representing standard tunnel operation fall closely to the remaining weak / modest bluntness data, while increasing tunnel quietness causes the data of [8] to diverge further from the rest of the data in Fig. 6.

According to eq. (14), the weak and modest bluntness transition data (excluding the NASA quiet tunnel data) is plotted in Fig. 7 in the form Re_{xtrans} versus $(MRe_b^{0.9})$. Eq. (14) is also plotted along with a +/-50% error band.

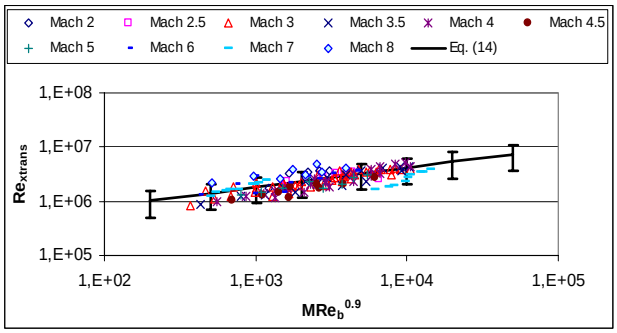

Fig. 7 Weak and modest bluntness data correlation – except [8]

Returning now to the presentation of Fig. 6, and equating eqs. (6) and (13) yields a threshold boundary between (combined) weak-modest and strong bluntness data at a value of $\mathrm{Re}_b \cong 1400M^2$. This boundary is significantly higher than the value of $\mathrm{Re}_b \cong 1000M^2$ that was assumed (and closely confirmed) in Fig. 2 as the boundary between (purely) modest and strong bluntness data.

Consequently, modest bluntness data are distinguished from strong bluntness data in Fig. 6 at the higher value of $(Re_b/M^2)=1400$, and this in turn, influences the strong bluntness data correlation, which takes a somewhat different form than eq. (6):

$$M\frac{x_{tr}}{b} = 7\cdot 10^6\left(\frac{\mathrm{Re}_b}{M^2}\right)^{-1.21} \qquad (15)$$

Eq. (15) is plotted in Fig. 6 with a +/-25% band that again encompasses all strong bluntness data.

Alternatively, eq. (15) may take the form:

$$\mathrm{Re}_{xtrans} = 7\cdot 10^6 M^{1.42}\,\mathrm{Re}_b^{-0.21} \qquad (16)$$

which is very similar to the original strong bluntness result, eq. (7). Notably, the strong bluntness data exhibits a significant stabilizing Mach number effect throughout.

4.3 Global Data Correlation

Further to the foregoing discussion, it is now attempted to correlate the entirety of the data (that is weak, modest and strong bluntness data, but excluding the NASA quiet tunnel results of [8]) with a single mathematical form. Regression analysis on the data of Fig. 8 yields:

$$M\frac{x_{tr}}{b} = 200000\left(\frac{\mathrm{Re}_b}{M^2}\right)^{-0.75} \qquad (17)$$

with a significative majority of the data falling within the +/-50% band plotted in Fig. 7.

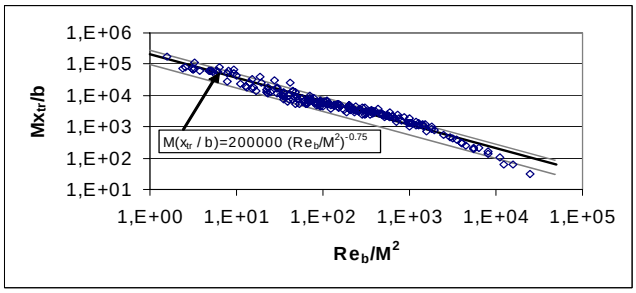

Fig. 8 Data correlation – all data except [8]

Equation (17) may take the following alternative form, also representing the entirety of the data considered herein:

$$\mathrm{Re}_{xtrans} = 200000M^{0.5}\,\mathrm{Re}_b^{0.25} \qquad (18)$$

According to eq. (18), the data of Fig. 8 is plotted in Fig. 9 in the form Re_{xtrans} versus (M^2Re_b). Eq. (18) is plotted with a +/-50% band.

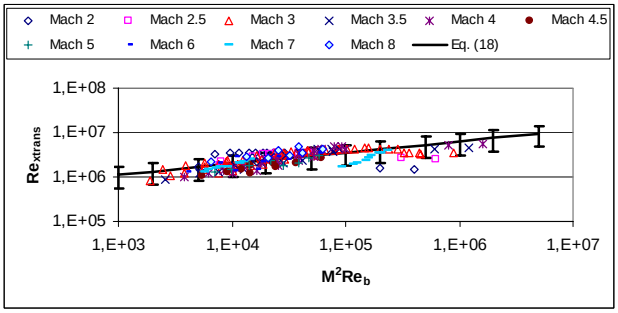

Fig. 9 Data correlation – all data except [8]

Evidently, expanding the data range to the limit of including also the strong bluntness data in a single global prediction formulation causes a significant deterioration to the quality of the correlation, particularly on the strong bluntness end of the data (where data availability is limited).

5 Summary and Conclusions

5.1 Data Summary

The available flat plate transition data is finally plotted in Fig. 10 for each Mach number, in the form Re_{xtrans} versus Re_b. The data is labeled as weak, modest or strong bluntness, according to the threshold boundary criteria of eqs. (9) and / or (10). Referring to Fig. 10, flat plate transition behavior may be summarized as follows:

- Increasing leading edge bluntness Reynolds number, Re_b, has an apparent stabilizing effect on weak and modest bluntness cases.
- At the low end of Re_b (weak bluntness cases), enhanced stability is observed. This is increasingly so with decreasing leading edge thickness or, differently said, for each weak bluntness data set and Mach number, transition Reynolds number increases with unit Reynolds number (in effect independent of leading edge thickness), as shown in Fig. 5.
- The inconsistent behavior of the four data sets in Fig. 5, and the lack of correlation for the constant A in eq. (11) present strong indications that weak bluntness transition is significantly influenced by parameters not modeled herein, such as initial disturbance environment (see NASA quiet tunnel data) and boundary layer receptivity (see Mach 8 data enhanced stability).
- The threshold Re_b boundary between weak and modest bluntness (i.e. between viscous- and bluntness-dominated) transition increases with Mach number approximately as per eq. (9). However, this is not a clearly defined boundary but rather a buffer zone, likely because of the influence of initial disturbances, receptivity and other parameters not included in the present analysis[4].
- In modest bluntness cases, the dominant parameter is clearly Re_b, as confirmed in Fig. 3. Increasing leading edge bluntness Reynolds number has a definite stabilizing effect on transition Reynolds number, which is only weakly dependent on Mach number and the actual leading edge thickness (or data source).
- Towards the end of the modest bluntness regime, there is a flattening of the transition Reynolds number curve. The predicted transition Reynolds number at the plateau (corresponding to the threshold boundary between modest and strong bluntness transition) is shown in Fig. 10 for each Mach number.
- The threshold Re_b boundary between modest and strong bluntness data, as well as the corresponding transition Reynolds number (the plateau level in Fig. 10), increase with Mach number, the former as per eq. (10), illustrated in Fig. 2, and the latter as per eq. (4) or eq. (7), when substituting eq. (10) for Re_b.
- Thereafter, increasing leading edge bluntness Reynolds number, Re_b, has a mild destabilizing effect (transition reversal) on strong bluntness cases, whereas increasing Mach number has a strong stabilizing effect (illustrated in Fig. 4 and by eqs. (7) and (8)).

5.2 Correlation Summary

5.2.1 Weak Bluntness Data

Following the preceding discussion, weak bluntness transition Reynolds number is dominated by the unit Reynolds number, and correlates in the form of eq. (11):

$$\mathrm{Re}_{xtrans} = A\,\mathrm{Re}_{unit}^{k} \qquad (11)$$

Within the limited available data, the exponent k correlates with the Mach number as per eq. (12); however, the lack of a simple correlation for the

[4] For example, some very stable NASA quiet tunnel data points are labeled as modest bluntness data in Fig. 10, while some Mach 3-5 data are labeled as weak bluntness data when they correlate reasonably well with the rest of the modest bluntness data.

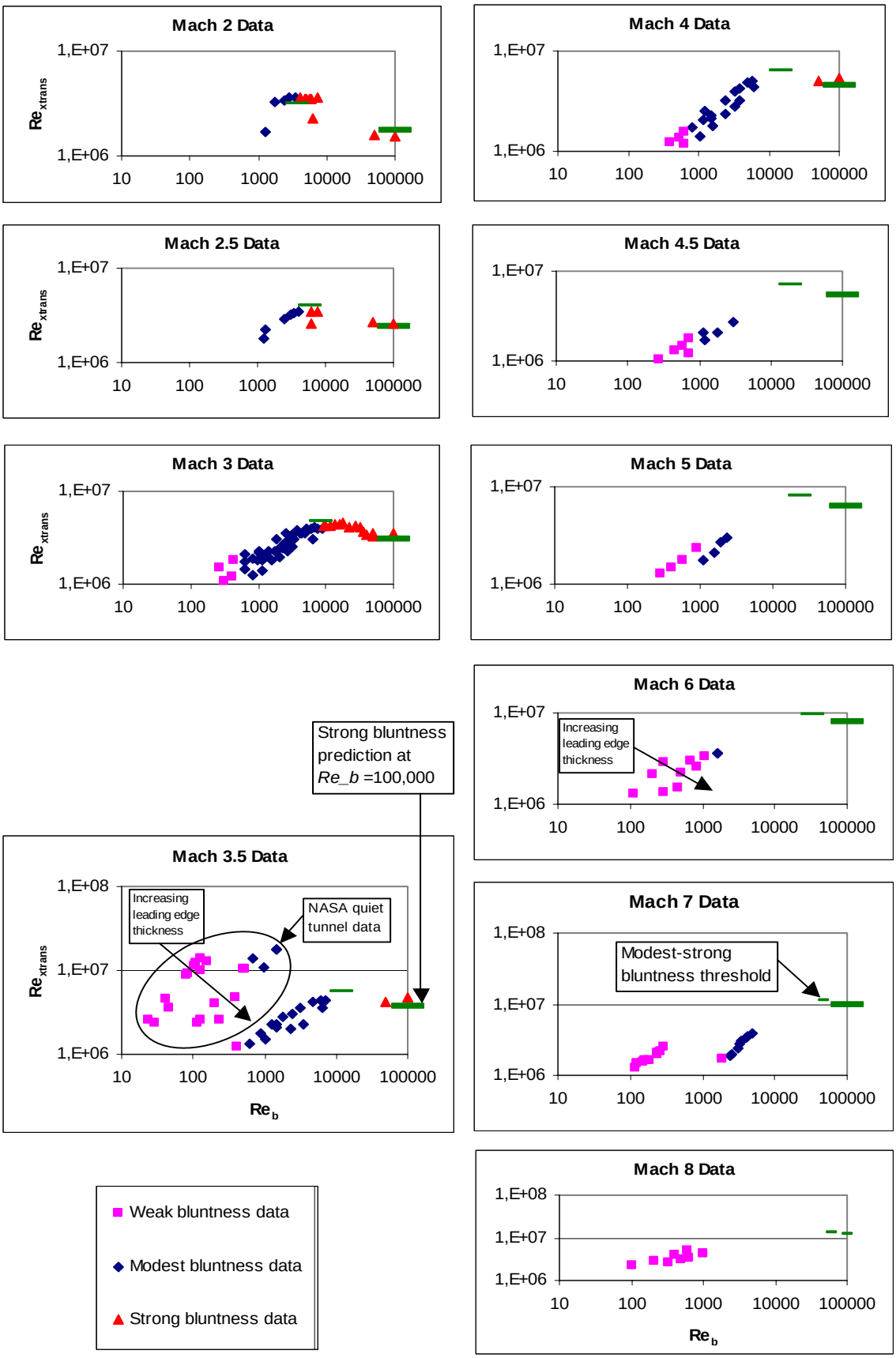

Fig. 10 Data summary Re_{xtrans} versus Re_b – Mach number as a parameter

constant A suggests an important influence of the initial disturbance environment and, possibly, boundary layer receptivity.

Consequently, the best correlation form achieved so far for weak bluntness data is eq. (14) established for the combined weak and modest bluntness data:

$$\mathrm{Re}_{xtrans} = 150000 M^{0.36} \mathrm{Re}_b^{0.32} \qquad (14)$$

which is reasonably good (typically +/-50%) for all standard wind tunnel weak and modest bluntness data (Fig. 7). However, with reference to the NASA quiet tunnel data in Fig. 6, it is noted that increasing tunnel quietness has a pronounced stabilizing effect that is not captured by eqs. (13) or (14).

5.2.2 Modest Bluntness Data

Modest bluntness data correlate well (generally within +/-30%) according to eq. (4) or its reduced form eq. (5):

$$\mathrm{Re}_{xtrans} = 100000 \mathrm{Re}_b^{0.42} \qquad (5)$$

Notably, Mach number seems to have a very mild stabilizing effect on modest bluntness transition Reynolds number as per eq. (4).

5.2.3 Strong Bluntness Data

Strong bluntness data (though relatively limited in quantity, Mach number range and data sources) correlate very well according to eq. (7):

$$\mathrm{Re}_{xtrans} = 6 \cdot 10^6 M^{1.38} \mathrm{Re}_b^{-0.19} \qquad (7)$$

exhibiting a strong stabilizing influence of Mach number on transition Reynolds number, and a fairly mild destabilizing effect of bluntness Reynolds number (which is mostly evident in the low supersonic regime in Fig. 10).

References

[1] Simeonides G. Leading edge bluntness effects on flat plate boundary layer transition – compilation of high speed experimental data. ESA-ESTEC *Doc. YPA/1881/GS*, 1996.

[2] Simeonides G. Correlation of laminar-turbulent transition data over flat plates in supersonic / hypersonic flow including leading edge bluntness effects. *Shock Waves*, Vol.12, No.6,pp.497-508,2003.

[3] Heffner K and Arnal D. Leading edge bluntness effect on laminar-turbulent boundary layer transition on a flat plate at Mach 7. CERT-ONERA *RT-93/5618.98*, 1994.

[4] Cazenave F. Etude numerique des effets de l' emoussement de plaques planes sur la transition en ecoulement supersonique et hypersonique. Ph.D. Thesis, ENSAE, 1993.

[5] Simeonides G. Hypersonic shock wave boundary layer interactions over compression corners. Ph.D. Thesis, von Karman Institute / Univ. Bristol, 1992.

[6] Boerrigter HL, Charbonnier JM and Elbay MK. Quantitative boundary layer transition measurements on flat plates and cones in hypersonic flow. *EUROMECH 312*, VON Karman Institute Preprint 1994-05, 1993.

[7] Boerrigter HL and Charbonnier JM. On the effect of flowfield non-uniformities on boundary layer transition in hypersonic flow. *EUROMECH 330*, von Karman Institute Preprint 1995-19, 1995.

[8] Chen FJ, Malik MR and Beckwith IE. Boundary layer transition on a cone and flat plate at Mach 3.5. *AIAA Journal*, Vol. 27, No. 6, pp. 687-693, 1989.

[9] Maslov AA et al. Hypersonic boundary layer stability and transition. ITAM Report (communicated by Aerospatiale Espace et Defense to ESA/ESTEC in the frame of the 1994-1996 ESA TRP program on transition), 1994.

[10] Potter JL and Whitfield JD. Effects of unit Reynolds number, nose bluntness and roughness on boundary layer transition. *AEDC-TR-60-5*, 1960.

[11] Stetson KF, Kimmel RL, Thompson ER, Donaldson JC and Siler LG. A comparison of planar and conical boundary layer stability and transition at a Mach number of 8. *AIAA 22nd Fluid Dynamics, Plasma Dynamics and Lasers Conference*, Honolulu, AIAA Paper 91-1639, 1991.

[12] Pate SR and Groth EE. Boundary layer transition measurements on swept wings with supersonic leading edges. *AIAA Journal*, Vol. 4, No. 4, pp. 737-738, 1996.

[13] Jillie DW and Hopkins EJ. Effects of Mach number, leading edge bluntness and sweep on boundary layer transition on a flat plate. *NASA TN D-1071*, 1961.

[14] Arnal D. Laminar-turbulent transition problems in supersonic and hypersonic flows. *Aerothermodynamics of Hypersonic Vehicles,* AGARD-FDP / VKI Special Course, 1988.

[15] Stetson KF. Hypersonic boundary layer transition. *3rd Joint Europe / U.S. Short Course in Hypersonics*, Univ. Aachen, 1990.

[16] Malik MR, Spall RE and Chang C-L. Effect of nose bluntness on boundary layer stability and transition. *AIAA Paper 90-0112, 28th Aerospace Sciences Meeting,* Reno, 1990.